

Frequency Correlations of QPOs Based on a Disk Oscillation Model in Warped Disks

Shoji KATO

Department of Informatics, Nara Sangyo University, Ikoma-gun, Nara 636-8503

kato@io.nara-su.ac.jp, kato@kusastro.kyoto-u.ac.jp

and

(Received 2006 0; accepted 2007 0)

Abstract

In previous papers we proposed a model that high-frequency quasi-periodic oscillations (QPOs) observed in black-hole and neutron-star X-ray binaries are disk oscillations (inertial-acoustic and/or g-mode oscillations) resonantly excited on warped disks. In this paper we examine whether time variations of the QPOs and their frequency correlations observed in neutron-star X-ray binaries can be accounted for by this disk-oscillation model. By assuming that a warp has a time-dependent precession, we can well describe observed frequency correlations among kHz QPOs and LF QPOs in a wide range of frequencies.

Key words: accretion, accretion disks — quasi-periodic oscillations — resonance — neutron stars — warp — X-rays; stars

1. Introduction

Low-mass X-ray binaries (LMXBs) often show quasi-periodic oscillations (QPOs) in their X-ray flux. In the case of high-frequency QPOs (HF QPOs) in black-hole sources, they often appear in a pair and their frequencies are kept with time with the frequency ratio of 3 : 2. In the case of kHz QPOs in neutron-star X-ray sources, they frequently appear also in pair, but with time variation. The frequency ratio is not kept to 3 : 2. However, the time variations of the pair kHz QPOs are not only correlated each other, but also correlated with the time variation of low-frequency QPOs (LF QPOs) (Boutloukos et al. 2006). The purpose of this paper is to examine whether these correlated time-variations of QPOs in neutron-star X-ray binaries can be described as disk oscillations resonantly excited on warped disks.

In disks deformed by some external forces, excitation of disk oscillations by resonant processes is generally expected. A well-known example is the tidal instability in cataclysmic variables (Whitehurst 1988; Hirose and Osaki 1990; Lubow 1991). Another example is the excitation of spiral pattern in ram-pressure-deformed galactic disks (Tosa 1994; Kato and Tosa

1994). In the context of high-frequency QPOs, a warp will be one of the most conceivable deformations of disks. Based on this, we proposed a model that HF QPOs in black-hole X-ray binaries and kHz QPOs in neutron-star X-ray binaries are disk oscillations resonantly excited on disks deformed by warp (e.g., Kato 2003, 2004a,b; Kluźniak et al. 2004; Kato 2005a,b; Kato and Fukue 2006).

In this warp model there are three possible combinations of i) type of resonance and ii) type of oscillations. Stability analyses for these three cases show that inertial-acoustic oscillations and/or g-mode oscillations are excited by their horizontal coupling with a warped disks (Kato 2004b). An overview of the resonant non-linear coupling processes among oscillations and warp, which feedback to the original oscillations so as to amplify or dampen the oscillations, are shown in figure 1 of Kato (2004b). By this resonant model in warped disks, we can account for the 3 : 2 frequency ratio of HF QPOs in black-hole X-ray sources (e.g., Kato 2004b; Kato and Fukue 2006).

Although the above analyses of stability by Kato (2004b) is only to the case in which the warp has no precession, we think that the excitation of inertial-acoustic oscillations and/or g-mode oscillations still holds even in the case in which the warp has precession. We further assume that the warp has time-dependent precession in the case of neutron stars.¹ By the time-dependent precession, the resonant radius changes with time. Hence, frequencies of resonant oscillations vary with time. During the frequency changes of resonant oscillations, they are correlated each other in this warp model as shown below, since the resonance occurs at the same radius for different oscillation modes.

In this paper we demonstrate that the observed correlations of kHz QPOs and LF QPOs in neutron-star X-ray binaries can be described by this warp model with time-dependent precession.

2. Overview of the Resonant Oscillation Model in Warped Disks

We present here the main part of the warp model, although the model has various variations. Let us consider disk oscillations described by (ω, m, n) , where ω and m are angular frequency and azimuthal wavenumber ($m = 0, 1, 2, \dots$) of the oscillations, respectively, and n is an integer ($n = 0, 1, 2, \dots$) describing node number of the oscillations in the vertical direction (e.g., see Kato et al. 1998; Kato 2001). For a set of (ω, m, n) , there are two different kinds of modes of oscillations, except for the case of $n = 0$. In the case of $n = 0$, we have inertial-acoustic oscillations alone, while in the case of $n \geq 1$ we have two different modes of oscillations. One is gravity mode, and the other is corrugation mode ($n = 1$) or vertical-acoustic mode ($n \geq 2$) (see

¹ In the case of black-hole sources we assume that the warp has no precession. This difference will be related to the difference of the surface of the central sources. If the surface is present, magnetic couplings and radiative couplings (e.g., Pringle 1996; Maloney et al. 1996) of the disks with the central sources will cause precession of warps.

Kato et al. 1998; Kato 2001).

Now, the disks are assumed to be warped with a time-dependent precession. The warp is a kind of a global one-armed corrugation waves, and is described by $(\omega_p, 1, 1)$, where ω_p is the angular frequency of the precession, $\omega_p > 0$ being prograde and $\omega_p < 0$ retrograde.

2.1. Resonant condition and resonant radius

Nonlinear resonant interaction between a warp with $(\omega_p, 1, 1)$ and an oscillation with (ω, m, n) brings about oscillations described by $(\omega \pm \omega_p, m \pm 1, n \pm 1)$, where arbitrary combinations of \pm are possible. (These oscillations are called hereafter intermediate oscillations.) These intermediate oscillations have resonant interaction with the disk at particular radii where the dispersion relation of the intermediate oscillations is satisfied. There are two kinds of resonance, corresponding to the fact that two kinds of oscillation modes are described by the same dispersion relation, i.e., i) inertial-acoustic oscillations and gravity oscillations, and ii) vertical-acoustic oscillations. We call the resonance related to the former oscillations horizontal resonance, while the resonance related to the latter oscillations vertical resonance (e.g., see Kato 2004b).

After making the resonant interaction with the disk, the intermediate oscillations nonlinearly couple with the warp to feedback to the original oscillations (ω, m, n) (see figure 1 of Kato 2004b). This nonlinear feedback processes amplify or dampen the original oscillations, since a resonance process is involved in the feedback processes. Careful stability analyses which resonance excites oscillations and which oscillations are excited have been made in the case of no precession (Kato 2004b). The results show that inertial-acoustic oscillations and/or gravity oscillations are excited by horizontal resonance (Kato 2004b). This result will not change even when there is precession. Hence, we hereafter restrict our attention only on the above case, i.e., inertial-acoustic oscillations and/or gravity oscillations which have resonant interaction with the warped disk through the horizontal resonance.

For the resonance to occur effectively, the place of resonance and the place where the oscillations predominantly exist must be the same. We find that in the case of no precession, the condition is realized at the radius of $\kappa = \Omega/2$, where κ is the epicyclic frequency and Ω is the angular velocity of disk rotation. This can be simply extended to the case where the warp has precession, which gives the resonant condition as [see also Kato (2005a)²]

$$\kappa = \frac{1}{2}(\Omega + \omega_p). \quad (1)$$

Hereafter, Ω is taken to be the Keplerian angular velocity, Ω_K , when numerical figures are necessary. Equation (1) gives the resonant radius, r_r , as a function of ω_p , when the mass and spin of central source are given. The r_r - ω_p relation is shown in figure 1 for the case in which the mass of the central source is $2M_\odot$ and the central source has no spin (i.e., the metric is the

² In Kato (2005), $\omega_p > 0$ was retrograde, but here we adopt $\omega_p >$ for prograde precession.

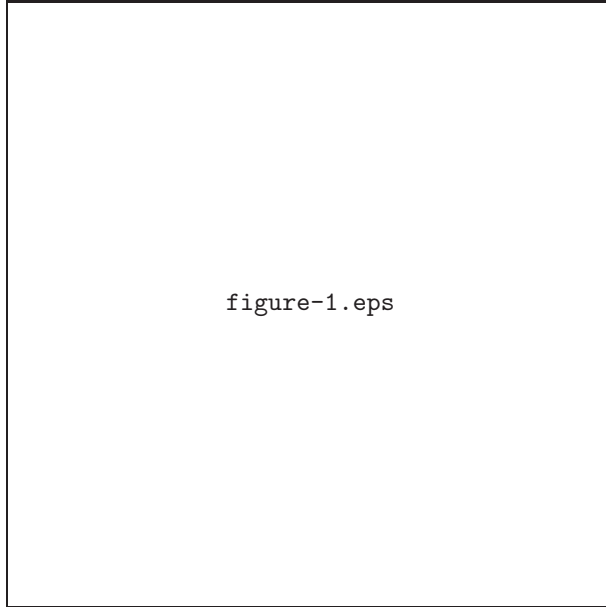


Fig. 1. The resonant radius versus frequency of precession. The mass of the central source is $2M_{\odot}$. The metric is taken to be the Schwarzschild, i.e., $a_{*} = 0$. In disks in which the warp has no precession, the resonance occurs at $4r_{\text{g}}$. When the precession is prograde ($\omega_{\text{p}} > 0$), the resonant radius becomes smaller than $4r_{\text{g}}$ as the precession frequency increases, while it becomes larger when the precession is retrograde ($\omega_{\text{p}} < 0$) and its absolute value increases. In the case of retrograde precession, however, the resonant radii are not unique for a given ω_{p} , as shown in the figure. That is, another resonance (resonance at an outer radius) appears far outside of the disk. The radius of the outer resonance moves inward, as the absolute value of precession increases. The inner and outer resonances join together for a certain value of retrograde precession, and no resonance occurs for a larger value of retrograde precession.

Schwarzschild one). It is noted that when the mass of the central source is smaller than $2M_{\odot}$ by a factor α , the same $r_{\text{r}}/r_{\text{g}}$ is realized for the precession faster than that in the case of $2M_{\odot}$ by factor α^{-1} .

The resonant condition in the case of no precession, $\kappa = \Omega/2$, is realized at $4r_{\text{g}}$ when there is no spin. Figure 1 shows that if the precession is prograde, the resonant radius becomes smaller than $4r_{\text{g}}$ with increase of precession frequency, ω_{p} . If the precession is retrograde, however, we have resonance at two different radii. One is close to $4r_{\text{g}}$ when the precession is small, and moves outward with increase of the absolute value of ω_{p} . The other one is far outside of the disk when the precession is weak, and the radius of resonance moves inward with increase of the absolute value of precession. At a certain value of retrograde precession, both radii coincide and no resonance occurs for retrograde precession with faster precession.

2.2. frequencies of resonant oscillations

Since inertial-acoustic oscillations or g-mode oscillations are concerned here, the place where the oscillations exist predominantly is the place where $(\omega - m\Omega)^2 - \kappa^2 \sim 0$ is satisfied (e.g., see Kato and Fukue 2006). In other words, frequencies of resonant oscillations are $(m\Omega \pm$

$\kappa)_r$, where various m 's are allowed, and the subscript r denotes the values at the resonant radius. The axisymmetric oscillations with $m = 0$ will be observationally less interesting by the nature of symmetry itself. Hence we consider only non-axisymmetric oscillations. Typical non-axisymmetric modes of the oscillations are those with $m = 1$ and $m = 2$. Hence, as the frequencies of such oscillations, we have $(\Omega - \kappa)_r$ (i.e., $m = 1$), $(2\Omega - \kappa)_r$, (i.e., $m = 2$), $(\Omega + \kappa)_r$ (i.e., $m = 1$), $(2\Omega + \kappa)_r$ (i.e., $m = 2$),... For convenience, we introduce the following notations defined by

$$\omega_{LL} = (\Omega - \kappa)_r, \quad \omega_L = (2\Omega - \kappa)_r, \quad \omega_H = (\Omega + \kappa)_r. \quad (2)$$

Here, the relation between frequencies of resonant oscillations and of the observed QPOs should be briefly discussed. In the case of black-hole X-ray binaries, we think that the one-armed oscillations with frequency ω_{LL} will be observed with the two-fold frequency, $2\omega_{LL}$, in addition to ω_{LL} itself by the following reasons (Kato and Fukue 2006). In black-hole sources, the high-frequency QPOs are observed only in the phase where the sources are at the steep power-law state (i.e., very high state) (Remillard 2005). In such states, the disk region where the QPOs are excited will be inside a compact hot torus, and the observed QPO photons are those which are Comptonized in the torus. In such cases, observed Comptonized high energy photon from one-armed oscillations ($m = 1$) will have two maxima during one cycle of the oscillations (see figures 2 – 4 of Kato and Fukue 2006). This means that $2\omega_{LL}$ will be observed with large amplitude (in many cases with an amplitude larger than that of the oscillation of ω_{LL}), since the oscillation is one-armed (Kato and Fukue 2006). Based on this consideration, we have suggested that the observed pair QPO frequencies in black hole sources are ω_L and $2\omega_{LL}$ (not ω_{LL}) (see, e.g., Kato 2004b; Kato and Fukue 2006).

Even in the case of neutron-star X-ray binaries, a similar situation may exist. Including this possibility, we regard ω_H , ω_L , $2\omega_{LL}$, and ω_{LL} as the main candidates of observed QPO frequencies in neutron stars.

2.3. Frequency-Frequency Relations

Frequencies ω_H , ω_L , $2\omega_{LL}$, ω_{LL} , and ω_p are given functions of the resonant radius r_r , spin parameter a_* , and the mass M of the central source. Hence, eliminating r_r from these expressions for the frequencies, we obtain relations among ω_H , ω_L , $2\omega_{LL}$, ω_{LL} , and ω_p . Parameters are a_* and M . Figure 2 shows the relations by taking ω_L as the abscissa in the case of $a_* = 0$ and $M = 2M_\odot$. The straight line of $\omega_L - \omega_L$ relation is also shown for comparison. This figure should be compared with figure 2.9 of van der Klis (2004). The latter shows observed frequency-correlations among various QPOs in neutron-star LMXBs. Comparison suggests that the observed frequency correlations of QPOs seem to be qualitatively described by the present disk oscillation model. More close comparison between observations and the model is made in the next section.

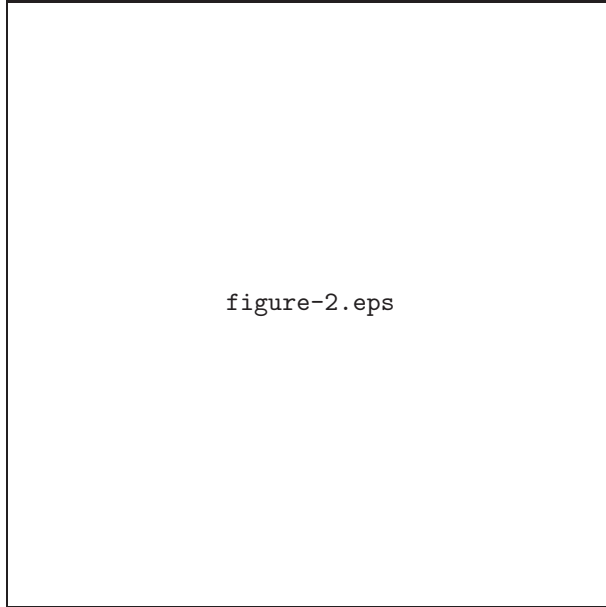


Fig. 2. Various frequencies as functions of ω_L . The frequency of precession shown here, ω_p , is the absolute value. In the main part of this figure, the value of ω_p is negative (retrograde). The values of parameters adopted here are $M = 2M_\odot$ and $a_* = 0$

3. Correlation of QPO Frequencies

3.1. Hectohertz QPOs

In atoll sources (less luminous neutron-star LMXBs), hectohertz QPOs (hHz QPOs) have been observed (see figure 2.9 of van der Klis 2004). Their frequencies are in the range of 100 – 200 Hz, and seen in atoll sources in most state. Their presence in Z sources is, however, uncertain. Different from kHz QPOs, their frequencies are approximately constant, which is similar across sources (van der Klis 2004).

The hectohertz QPOs can be interpreted in the present model as observations of warp. Figure 2 shows that for a wide range of variations of ω_L , ω_p is approximately constant around 100 – 200 Hz, which is consistent with the observational characteristics of hHz QPOs. The fact that the value of $|\omega_p|$ remains around 100 – 200 Hz is related to the fact that the lower limit of $\omega_p (< 0)$ shown in figure 1 is around 100 – 200 Hz. The lower limit of $\omega_p (< 0)$ depends on a_* . If $a_* > 0$, the maximum value of $|\omega_p|$ slightly decreases from that in the case of $a_* = 0$, while it increases with decrease of the mass of the central source.

3.2. Correlation of pair kHz QPOs

As argued in previous papers (e.g., Kato 2004b; Kato and Fukue 2006), we think that the high-frequency pair QPOs in black-hole LMXBs are oscillations of ω_L and $2\omega_{LL}$. Their frequency ratio is just 3 : 2, since we assume that in black-hole sources the warp has no

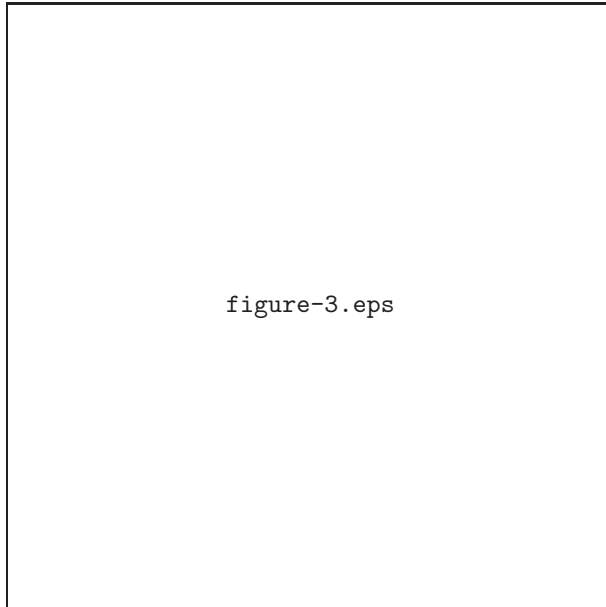


Fig. 3. Dependence of ω_H and ω_L on $2\omega_{LL}$ in the case of $a_* = 0$ and $M = 2.4M_\odot$. The plots of the upper versus lower frequencies of the observed pair kHz QPOs obtained by Bursa (2003) are superposed by taking the frequency of the lower kHz QPOs as $2\omega_{LL}$. This figure shows that the plots of the observed data are between two curves of $\omega_H - 2\omega_{LL}$ and $\omega_L - 2\omega_{LL}$. Bursa's diagram is taken from Abramowicz (2005).

precession.³ In the case of neutron-star LMXBs, we assume that the warp has time-dependent precession although the pair oscillations are still ω_L and $2\omega_{LL}$. We examine here whether the frequency correlation in kHz QPOs can be accounted for by this picture.

Figure 3 shows ω_L as a function of $2\omega_{LL}$ for $a_* = 0$ in the frequency range in which the ratio of the above two frequencies is around 3 : 2, i.e., the precession is not too large. For comparison, the $\omega_H - 2\omega_{LL}$ relation is also shown. In figure 3, the mass M of the central sources is taken so that $2\omega_{LL}$ becomes 600Hz in the case of no precession. This means that we have adopted $M = 2.4M_\odot$, since $2\omega_{LL}$ is given by $2\omega_{LL} = 1.43 \times 10^3 (M/M_\odot)^{-1}$ Hz in the case of $a_* = 0$ (e.g., see Kato and Fukue 2006).

Bursa (2003, see also Abramowicz 2005, Kluźniak 2005) plotted the observed data of pair QPOs of some typical neutron-star sources on a diagram of the upper kHz QPO frequency versus lower kHz QPO frequency, in order to see how their time changes are correlated. The plots obtained by Bursa have been superposed on figure 3 by regarding the lower QPO frequencies as $2\omega_{LL}$.

Figure 3 shows that the observed correlated changes of the upper and lower QPO frequencies are qualitatively described by the correlated changes of ω_L (or ω_H) and $2\omega_{LL}$.

³ The reason why there is a difference of disk precession in black-hole and neutron-star sources is a subject to be clarified, but we suppose that it will be related to the difference of surfaces of the central sources.

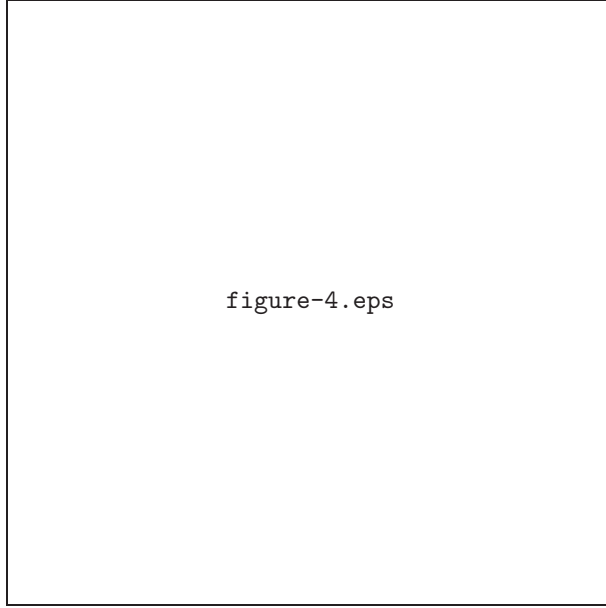


Fig. 4. Dependences of various frequencies of resonant oscillations on ω_{LL} . The frequencies considered here are in a low frequency range in order to compare them with those observed in Cir X-1. The most upper curve is the $(3\Omega + \kappa)_r - \omega_{LL}$ relation. Figure 6 of Boutloukos et al. (2006), which shows the observed frequency – frequency correlations in Cir X-1, has been superposed assuming that ν_{LF} corresponds to ω_{LL} .

3.3. *KHz QPOs in low frequency range and LF QPOs*

As shown in figure 1, resonance occurs at two different radii when precession is retrograde. One is close to $4r_g$, while the other is at an outer region. In some sources only the oscillations in the outer resonance will be observed, since the inner region of disks may be highly perturbed from the steady state by magnetic and/or radiative disturbances from the central source. Here, we consider characteristics of resonant oscillations which are excited at the outer resonant radius. In order to compare them with observational results, dependences of ω_H , ω_L , ω_p , and $2\omega_{LL}$ on ω_{LL} are shown in figure 4. In addition to them, the $(3\Omega + \kappa)_r - \omega_{LL}$ relation is drawn in figure 4, where $(3\Omega + \kappa)_r$ is the frequency of one of resonant oscillations with $m = 3$. There are other oscillation modes with high frequency. Among such oscillations, the oscillations of $(3\Omega - \kappa)_r$ (i.e., $m = 3$) have frequencies close to ω_H , and thus it is not shown here. Resonant oscillations with $(2\Omega + \kappa)_r$ are also not shown in figure 4, since the curve of the $(2\Omega + \kappa)_r - \omega_{LL}$ relation is between two curves of the $(3\Omega + \kappa)_r - \omega_{LL}$ and of the $\omega_H - \omega_{LL}$ relations. The straight line of $\omega_{LL} - \omega_{LL}$ is shown in the figure.

In order to examine whether the curves drawn in figure 4 can account for observational frequency-frequency correlations, the plots of observational data for Cir X-1 by Boutloukos et al. (2006) (figure 6 of their paper) are superposed on figure 4, assuming that the frequency of LF QPOs corresponds to ω_{LL} . The superposed figure seems to show that our disk oscillation model can well describe the observed frequency correlations. That is, ω_{LL} corresponds to the

frequency of LF QPOs and ω_L to that of the lower kHz QPOs. The frequency ω_H , however, seems to be slightly lower than the observed upper frequency of kHz QPOs. As frequencies of resonant oscillations whose frequencies are higher than ω_H , we have $(2\Omega + \kappa)_r$, $(3\Omega + \kappa)_r, \dots$ Among them, the frequency $(3\Omega + \kappa)_r$ seems to well describe the observed data of the upper kHz QPOs. The reason why oscillations of $(3\Omega + \kappa)_r$ dominate over those of $(2\Omega + \kappa)_r$ and ω_H is a subject to be discussed further.

When resonance occurs at an inner region of disks, $2\omega_{LL}$ is interpreted as the frequency of the lower kHz QPOs, as shown in figure 3. However, in the present case in which resonance occurs at an outer region, ω_{LL} (and $2\omega_{LL}$) is no longer the frequency of the lower kHz QPOs, since it is too low. It becomes the frequency of LF QPOs. The reason why ω_{LL} , not $2\omega_{LL}$, is the frequency of LF QPOs will be the followings. The outer region of the disk will not be covered with a hot torus. Thus, different from the case of black-hole X-ray sources, the resonant region will be outside a hot torus. In such case one-armed oscillations will be observed by the frequency of the oscillations themselves, not by two-fold ones. The inertial-acoustic oscillations with $m = 1$, however, propagate inward from the resonant radius (see the propagation region shown in figure 6 of Kato and Fukue 2006). Hence, if the oscillations propagate inward and enter into an hot torus, the oscillations of two-fold frequency will be observed (see Kato and Fukue 2006). This may be one of possible causes of the occasional appearance of the two-fold frequencies of ω_{LL} in Cir X-1.

In summary, the LF QPOs will be manifestation of the oscillations of ω_{LL} , and the lower kHz QPOs (ν_ℓ in notations of Boutloukos et al. 2006) will be a mixture of ω_p , ω_L , and ω_H . The upper kHz QPOs (ν_u in notations of Boutloukos 2006) are suggested to be oscillations of higher m modes such as those with $(3\Omega + \kappa)_r$ or $(2\Omega + \kappa)_r$.

4. Discussion

In this paper we have suggested that the pair kHz QPOs and the low-frequency QPOs in neutron-star LMXBs are qualitatively described, in a wide frequency range, as resonantly excited disk-oscillations in warped disks. The oscillations are non-axisymmetric inertial-acoustic or g-mode oscillations of $m = 1$, $m = 2$, and sometimes $m = 3$. Both inertial-acoustic oscillations and g-mode oscillations are possible candidates of QPOs, but the former will be better, since the magnitudes of temperature and density variations associated with the oscillations are larger in the former than in the latter. Especially, the oscillations of ω_{LL} will be inertial-acoustic oscillations, since they propagate inwards from the resonant radius and thus observational appearance of the harmonics, $2\omega_{LL}$, will be conceivable (see subsection 3.3).

In the present disk oscillation model, the cause of correlated frequency-changes of various QPOs is time change of resonant radius resulting from time-dependent precession of the warp. Has the warp been observed? We think that it has been observed as the hectohertz QPOs in atoll sources (see figure 2, in which ω_p is around 100 Hz \sim 200 Hz in a wide frequency range of

ω_L). Furthermore, in sources in which kHz QPOs appear in low frequency region, precession of the warp will be a cause of vertical spread of ν_ℓ in figure 4. The closeness of ω_p and ω_L in low frequency region comes from the following situation. The resonant condition, $\kappa = (\Omega + \omega_p)/2$ gives $\omega_p = (2\kappa - \Omega)_r$, which is $\sim \Omega_r$ when the resonant radius is far from the innermost region since there $\kappa \sim \Omega$. On the other hand, $\omega_L = (2\Omega - \kappa)_r \sim \Omega_r$ in such a region.

It is emphasized that by difference of frequency range in consideration, the counterparts of the oscillation modes to observed QPOs are different. That is, in the case in which the frequencies of kHz QPOs are high (subsection 3.2), the counterpart of the lower kHz QPOs is ω_{LL} (more exactly, $2\omega_{LL}$) (see figure 3). In the sources in which the frequencies of kHz QPOs are low (subsection 3.3), however, the counterpart of the lower kHz QPOs is ω_L , not ω_{LL} . In the latter case, the oscillation of ω_{LL} corresponds to ν_{LF} (see figure 4).

There are some problems to be examined or to be clarified further. First, it is known that the frequencies of lower kHz QPOs, ν_ℓ , and those of horizontal branch QPOs, ν_{HBO} , are correlated as $\nu_\ell \sim 0.08\nu_{HBO}$ (Psaltis et al. 1999; Belloni et al. 2002). In the framework of our present model, there are no oscillation modes corresponding to the horizontal branch QPOs. They might be related to resonant oscillations resulting from other types of resonance. Even in the framework of the resonant oscillation model in warped disks, there are other types of resonant oscillations (Kato 2004a; 2005b), although their excitation is uncertain. Second, a detailed inspection of figure 3 shows that the $\omega_L-2\omega_{LL}$ relation cannot always well describe the observed data. That is, to sources whose lower frequencies are lower than 600 Hz (i.e., GX 4340+0 and GX-5), the observed data are generally above the $\omega_L-2\omega_{LL}$ curve on the diagram, rather close to the $\omega_H-2\omega_{LL}$ curve. A preliminary study seems to show that it is difficult to explain the deviation by adjusting the values of parameters (mass and spin of the central source). If we want to explain the difference by a deviation of disk rotation from the Keplerian one, a rather large deviation is necessary. If ω_H is taken as the upper QPO frequency below 900 Hz and ω_L above 900 Hz, qualitative agreement with observations becomes better. However, it seems not to be clear whether such choice of oscillation modes is physically acceptable. Some more consideration concerning the cause of the deviation is necessary, which is a subject in the future.

References

- Abramowicz, M.A. 2005, *Astron. Nachr.* 326, No.9
 Belloni, T., Psaltis, D., van der Klis, M. 2002, *ApJ.*, 572, 392
 Boutloukos, S., van der Klis, M., Altamirano, D., Klein-Wolt, M., Wijnands, R., Jonker, P.G., Fender, R.P. 2006, *astro-ph/0608089*
 Bursa, M. 2003, unpublished
 Hirose, M., Osaki, Y. 1990, *PASJ* 42, 135
 Kato, S. 2001, *PASJ*, 53, 1

- Kato, S. 2003, PASJ, 55, 801
- Kato, S. 2004a, PASJ, 56, 559
- Kato, S. 2004b, PASJ, 56, 905
- Kato, S. 2005a, PASJ, 57, L17
- Kato, S. 2005b, PASJ, 57, 679
- Kato, S., Fukue, J., & Mineshige, S. 1998, Black-Hole Accretion Disks (Kyoto: Kyoto University Press)
- Kato, S., Tosa, M. 1994, PASJ, 46, 559
- Kato, S., Fukue, J. 2006, PASJ, 58, 909
- Kluźniak, W. 2005, Astron. Nachr. 326, 820
- Kluźniak, W., Abramowicz, M. A., Kato, S., Lee, W. H., & Stergioulas, N. 2004, ApJ, 603, L89
- Lubow, S.H. 1991, ApJ, 381, 259
- Psaltis, D., Belloni, T., van der Klis, M. 1999, ApJ., 520, 262
- Remillard, R.A. 2005, Astron. Nachr., 326, 804
- Tosa, M. 1994, ApJ, 426, L81
- van der Klis, M. 2004, in Compact stellar X-ray sources (Cambridge University Press), eds. W.H.G. Lewin and M. van der Klis (astro-ph/0410551)
- Whitehurst, R. 1988, MNRAS 232, 35